Symmetry and Self-Similarity with Coupled Logistic Maps

W. Metzler, W. Beau, W. Frees, and A. Ueberla
Interdisziplinäre Arbeitsgruppe Mathematisierung, Department of Mathematics,
University of Kassel, D-3500 Kassel, F.R. Germany

Z. Naturforsch. **42a**, 310–318 (1987); received September 24, 1986

The symmetric coupling of two one-dimensional logistic maps displays different types of symmetric and asymmetric attractors on its route to chaos. Coexisting attractors possess basins in the phase space with Julia-like boundaries. Even classical fractal boundaries occur, when the basins of the coupled map with complex variables are explored. The self-similar features of the objects obtain particular fascination by their symmetries dependent on the map.

1. Introduction

Much insight into the dynamics of non-linear systems has been gained through studies of discrete mappings. A canonical example of such mappings, which displays a period-doubling route to chaos, is the logistic map [1].

The two-dimensional map studied here is a "crosswise" symmetric coupling of two identical logistic maps. Related couplings of nonlinear oscillators have been discussed by Kaneko [2] as well as Hogg & Huberman [3]. They correspondingly found quasiperiodic behavior with frequency lockings as well as bifurcations into aperiodic behavior.

The present work should complete their results but sets up priorities on explorations of global attraction in the phase space and in the parameter space. We have considered the basins of coexisting periodic attractors which form stripe structures in a self-similar manner. Their separatrices are continuous Julia-like [4] sets. Corresponding self-similar features occur, when we study the level sets of equal attraction in the basins of low order cycles.

Further, in accordance with predictions of Roessler et al. [4], the map possesses a similar complexity in the parameter space. Neither here nor in the phase space our experiments resulted in classical fractal basin boundaries. But fractals occur for the "complex pendant" of the coupled logistic map, which is nothing else but a four-dimensional (real) map.

Reprint requests to Dr. W. Metzler, IAGM, Fachbereich Mathematik, Gh/Universität Kassel, Heinrich-Plett-Str. 40, D-3500 Kassel.

2. The Map

It is well known [5] that the iteration scheme

$$x_{k+1} = x_k + h\,x_k(1 - x_k)\,, \quad h > 0\,, \tag{1}$$

which is Euler's method for solving the logistic equation

$$\dot{x} = x(1 - x)\,,$$

may be transformed into

$$u_{k+1} = r\,u_k(1 - u_k)$$

with

$$u_k = (h/(1 + h))\,x_k\,, \quad r = 1 + h\,. \tag{2}$$

Forgetting that (1) is an approximation and treating h as a parameter which need not be small, the logistic map (2) is one of the most classical examples in the study of bifurcations and chaos of dynamical systems associated with interval maps [1, 6, 7, 8].

We study two logistic maps coupled cross-activatingly, that is,

$$\begin{aligned} u_{k+1} &= r\,u_k(1 - u_k) + (r - 1)\,v_k\,, \\ v_{k+1} &= r\,v_k(1 - v_k) + (r - 1)\,u_k\,. \end{aligned} \tag{3}$$

This map can be regarded as a simple model of two coupled systems each of which exhibits a period-doubling bifurcation route to chaos. Using the above transformation gives

$$\begin{aligned} x_{k+1} &= x_k + h\,(x_k - x_k^2 + y_k)\,, \\ y_{k+1} &= y_k + h\,(y_k - y_k^2 + x_k)\,. \end{aligned} \tag{4}$$

Relative to (4) the symmetry axis $x = y$ is an invariant manifold. Reduction of (4) onto $x = y$

0340-4811 / 87 / 0300-0310 $ 01.30/0. – Please order a reprint rather than making your own copy.

Dieses Werk wurde im Jahr 2013 vom Verlag Zeitschrift für Naturforschung in Zusammenarbeit mit der Max-Planck-Gesellschaft zur Förderung der Wissenschaften e.V. digitalisiert und unter folgender Lizenz veröffentlicht: Creative Commons Namensnennung-Keine Bearbeitung 3.0 Deutschland Lizenz.

This work has been digitalized and published in 2013 by Verlag Zeitschrift für Naturforschung in cooperation with the Max Planck Society for the Advancement of Science under a Creative Commons Attribution-NoDerivs 3.0 Germany License.

Zum 01.01.2015 ist eine Anpassung der Lizenzbedingungen (Entfall der Creative Commons Lizenzbedingung „Keine Bearbeitung") beabsichtigt, um eine Nachnutzung auch im Rahmen zukünftiger wissenschaftlicher Nutzungsformen zu ermöglichen.

On 01.01.2015 it is planned to change the License Conditions (the removal of the Creative Commons License condition "no derivative works"). This is to allow reuse in the area of future scientific usage.

results in the one-dimensional iteration scheme

$$x_{k+1} = x_k + h(2x_k - x_k^2), \tag{5}$$

which can be transformed into (2) by

$$u_k = (h/(1+2h))\, x_k \quad \text{and} \quad r = 1 + 2h. \tag{6}$$

Kaneko [2] as well as Hogg and Huberman [3] investigated the transition to chaos of coupled logistic maps with linear coupling terms of the form $d \cdot (x_k - y_k)$. They demonstrated transition from quasiperiodicity to chaos accompanied by frequency lockings with symmetry breaking. Kaneko also found self-similar stripe structures formed by the basins of coexisting attractive cycles. Related transitions to chaotic behavior of coupled nonlinear mappings have also been studied in [9, 10, 11].

3. Transition to Chaos

The map (4) can be derived from Kaneko's equations by a linear change of coordinates. But in this paper we consider another bifurcation parameter than he did. First, we give some analytical properties of (4). There are two fixed points, (0, 0) and (2, 2). The origin is unstable, and the point (2, 2) is a sink for $0 < h \leqq 0.5$ and unstable for $h > 0.5$. A hyperbolic 2-cycle

$$O_h = \{(x_h, y_h), (y_h, x_h)\} \quad \text{with} \tag{7}$$
$$x_h = (1 + (2h-1)^{1/2})/h\,, \quad y_h = (1 - (2h-1)^{1/2})/h$$

is born in (2, 2) at $h = 0.5$ and moves for $h \to \infty$ to (0, 0) on a circle given by

$$(x_h - 1)^2 + (y_h - 1)^2 = 2\,. \tag{8}$$

This can be derived easily from (4), when inserting x_h and y_h. Moreover, O_h is stable for $0.5 < h < 0.6$ and unstable for $h > 0.6$. The stability of O_h is determined by the Jacobian $DF_h^2(x_h, y_h)$, or equivalently $DF_h^2(y_h, x_h)$, of the second iterate of

$$F_h(x, y) = (x + h(x - x^2 + y), y + h(y - y^2 + x)) \tag{9}$$

given by (4). For $h > 0.5$, (x_h, y_h) and (y_h, x_h) are fixed points of F_h^2. The Jacobian of F_h^2 is given by

$$DF_h^2(x_h, y_h) = \begin{pmatrix} 5 - 10h + 2h^2 & 4h(2h-1)^{1/2} - 2h + 2h^2 \\ -4h(2h-1)^{1/2} - 2h + 2h^2 & 5 - 10h + 2h^2 \end{pmatrix}; \tag{10}$$

its eigenvalues are

$$\lambda_h = 5 - 10h + 2h^2 \pm (20h^2 - 40h^3 + 4h^4)^{1/2}. \tag{11}$$

Analyzing the roots of the radicant yields $|\lambda_h| < 1$ for $h < 0.6$, $|\lambda_h| = 1$ for $h = 0.6$ and $|\lambda_h| > 1$ if $h > 0.6$.

Further,

$$\left.\frac{\mathrm{d}\,|\lambda_h|}{\mathrm{d}h}\right|_{h=0.6} = 10 \tag{12}$$

indicates [12, p. 162] that the 2-cycle O_h loses its stability via a Hopf bifurcation and a 2-torus appears. 2-torus means that the second iterated map gives a single torus or loop (see [2]).

Kaneko [2] found for the coupled logistic map transition from a 2-torus to chaos with frequency lockings. According to his results, numerical experiments at increasing values of h show quasiperiodic motion with complicated transitions. For $h > 0.6$, the loops grow accompanied by frequency lockings, overlap themselves and finally reach a structure looking like the Eiffel tower (Fig. 1) at $h = 0.684$. Several period doubling sequences can be observed in the locking states. One of them starts at 0.65955 with period 13 (cf. Fig. 2), doubles at 0.65966 to period 26 and can still be observed at 0.6597298 with period 1664. The largest Lyapunov exponent, given by [3]

$$\lambda = \lim_{n \to \infty} 1/n \ln(\| DF_h^n(x_0, y_0) \|) \tag{13}$$

for an initial point (x_0, y_0), becomes positive at $h \approx 0.651$ when overlapping begins. The chaotic attractor is completely developed (Fig. 1) about $h = 0.684$ [13], where $\lambda = 0.1534$. The chaotic region is followed by escape which can be observed for $h \gtrsim 0.686$ (see Figure 2). For these calculations we took 50 000 iterations from the initial values $x_0 = 0.4$ and $y_0 = 0.5$.

4. Phase Space and Julia Boundaries

In this section we study similarity structures which are produced by the basins of coexisting periodic attractors. First, we note that the set of all

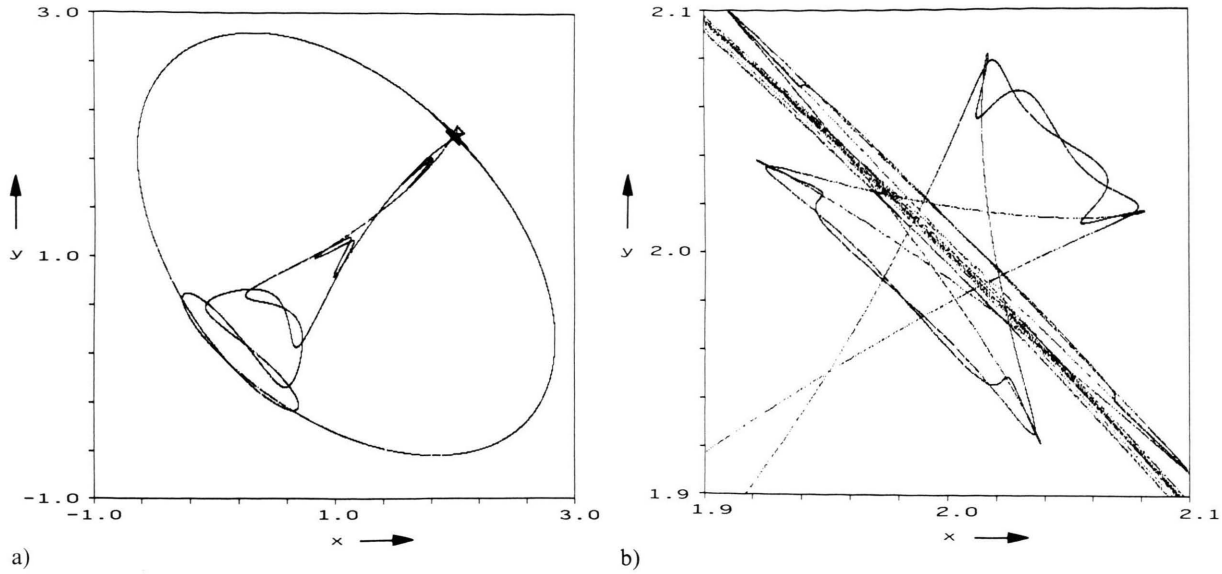

Fig. 1. (a) Chaotic attractor of (4) at $h = 0.684$ in the region $[-1, 3]\times[-1, 3]$. 30 000 iterations (200 dark) have been taken with double precision arithmetic from the initial point (0.4, 0.5). – (b) Blow-up of the region $[1.9, 2.1]\times[1.9, 2.1]$ in Fig. 1 (a).

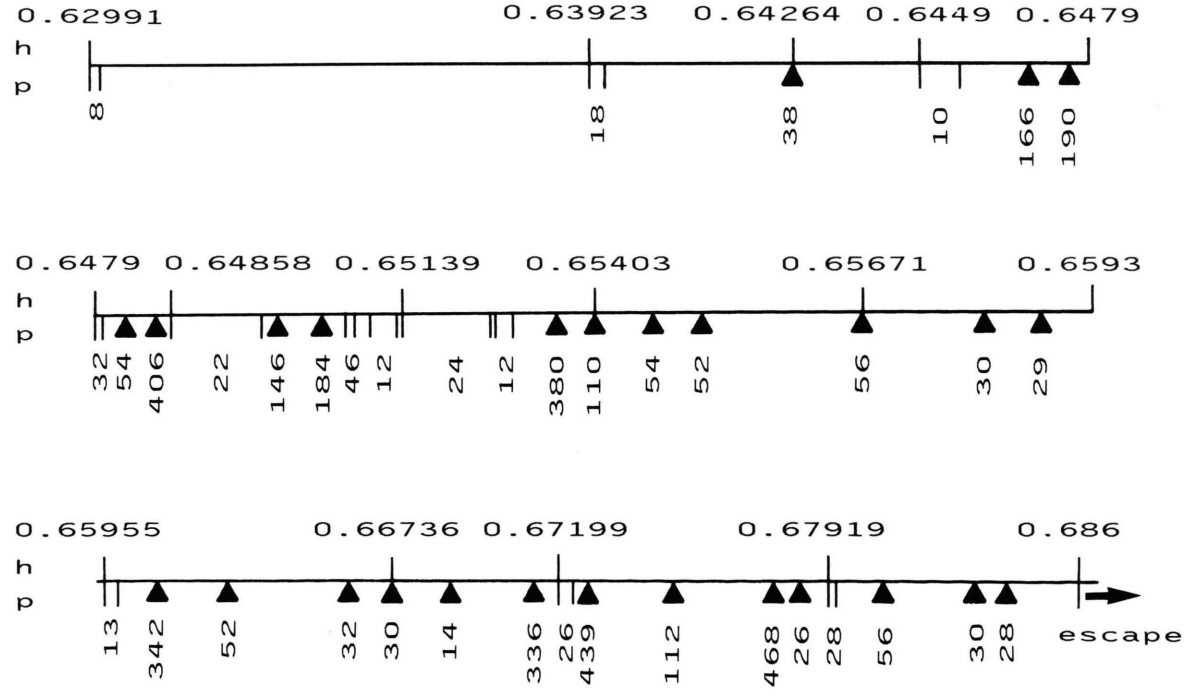

Fig. 2. A rough phase diagram of the coupled logistic map. Periods(p) have been plotted according to the following convention: Initially, the point (0.2, 0.4) is iterated 5000 times. The next iterates are stored, the first of them is taken as test point. If a subsequent iterate is closer than 10^{-5} to the test point, a period is assumed. This assumption is accepted, if all members of the next 100 orbits are closer than 10^{-3} to the corresponding stored points.

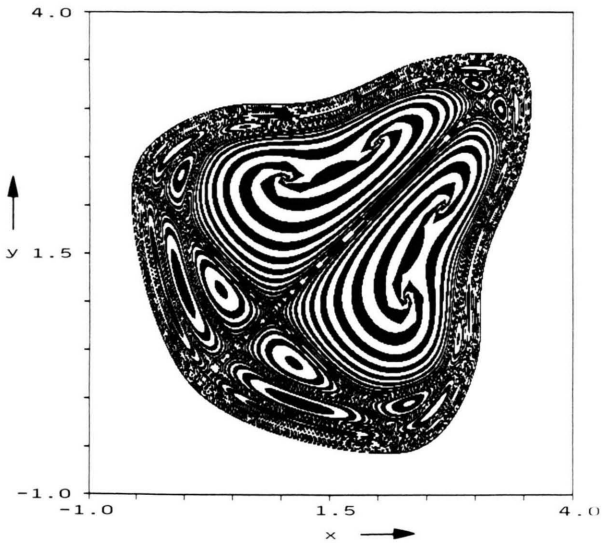

Fig. 3. Decomposition of the basin of the period-2 orbit (7) for $h = 0.58$ into level sets of equal attraction. Colouring convention: Picture elements (pixels) representing the initial values in the plotted region $[-1, 4] \times [-1, 4]$ are painted black, if their iterates hit a pixel mask of the attractor at an odd number of iterations. Otherwise they remain white.

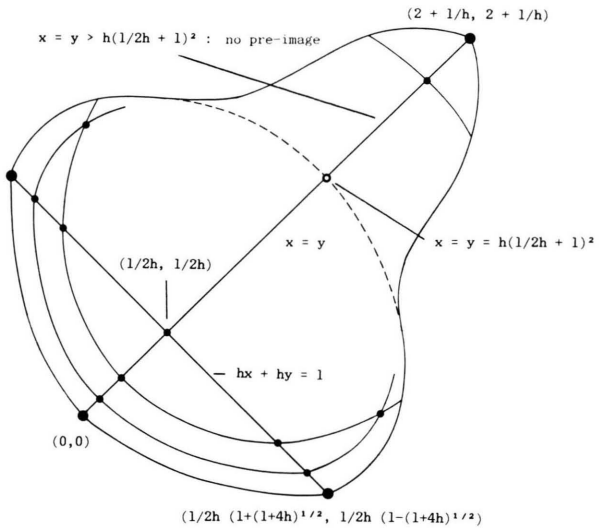

Fig. 4. Schematic representation of the skeleton given by (17). For discussion see text.

initial points (x_0, y_0) with bounded iterates under the map (4) looks like a pear (see Fig. 3) for all $h > 0$ till escape. It changes its shape slightly with h. Figure 3 shows a decomposition of the basin of the 2-cycle (7) for $h = 0.58$ into level sets of equal attraction. Picture elements representing the initial values in the plotted region, whose iterates hit the attractor at an odd number of iterations, are painted black. Otherwise, they remain blank. The resulting pattern is symmetric about $x = y$. It resembles the decomposition of the "pear" into the basins of two coexisting periodic attractors which are mirror images of each other about $x = y$ (cf. Figure 5 (a)).

This Julia-like [4, 14] "speed pattern" of the pear loses its clarity, when we increase the parameter h. This is due to the fact, that for $h > 0.6$ high order periodic, quasiperiodic and chaotic motion appears. But the "skeleton" of the pear (Fig. 4) persists for all values of $h > 0.5$ until escape.

Next, we study this skeleton. First, we note that all points of the upper part of the pear (see Fig. 4) have no (real) pre-image. Especially, on the symmetry axis these are the points

$$x = y > h(1/2\,h + 1)^2 . \tag{14}$$

Regarding (6), this corresponds to the fact that the one-dimensional map (2) has no real pre-image for $u > r/4$. Defining

$$S_{h,0} = \{(x, y) \mid 0 < x = y \leqq h(1/2\,h + 1)^2\}, \tag{15}$$

the "ribs" of the skeleton in Fig. 4 are given by

$$S_{h,n} = \{(x, y) \mid F_h^n(x, y) \in S_{h,0}\}, \tag{16}$$

where F_h^n is the n-th iterate of (9). Obviously, $S_{h,n} \subset S_{h,n+1}$, and the whole skeleton is given by

$$S_h = \bigcup_{n \geqq 0} S_{h,n} . \tag{17}$$

Especially, all points of intersection of the ribs are mapped onto $(1/2\,h, 1/2\,h)$, and the pear's part of the line $h\,x + h\,y = 1$ is mapped onto the diagonal's $0 < x = y \leqq h(1/2\,h + 1)^2$ by one iteration step. Additionally, in the limit we get

$$\lim_{k \to \infty} F_h^k(S_{h,n}) = \{(2, 2)\} \quad \text{for} \quad n \geqq 0 \tag{18}$$

from the one-dimensional map (6) which has a stable fixed point for $h \leqq 1$, that is, $r = 2\,h + 1 \leqq 3$. Thus, all points of the skeleton (17) of the pear converge to the fixed point (2, 2) for all interesting

values of the parameter h. Analogously, we can deduce that all boundary points of the pear tend to the origin.

If the coupled map (4) has two or more coexisting attractors, the pear decomposes into different basins of attraction. We shall discuss now two typical cases, $h = 0.645$ and $h = 0.678$.

For $h = 0.645$, there are two stable period-10 orbits coexisting; for the eigenvalues of the 10-th iterated linearized map we compute $|\lambda_1| \approx 6.5490638495 \cdot 10^{-1}$ and $|\lambda_2| \approx 2.7577337437 \cdot 10^{-3}$. Their basins of attraction are antisymmetric about $x = y$ in the sense that if the point (x_0, y_0) belongs to the basin of one period-10 orbit, the point (y_0, x_0) belongs to the basin of the other $p = 10$ orbit (Figure 5). This is due to the fact that the map (4) is symmetric and the two $p = 10$ orbits are mirror images of each other about $x = y$.

Numerical approximations of the basin boundaries indicate the existence of further two but unstable ($|\lambda_1| \approx 1.344916$, $|\lambda_2| \approx 2.903783 \cdot 10^{-3}$) period-10 orbits (cf. Figure 6). Their common basin of attraction is exactly the separatrix of the basins of the two stable 10-cycles. Each component of this separatrix is part of the basin of exactly one of the two unstable orbits, two neighboring components belong to different orbits.

The separatrix, i.e. the basin boundary for the two period-10 attractors of Fig. 6, is a continuous Julia set. Roessler et al. [14] predicted it with reference to [13] to be the first explicit example of Julia-like boundaries in a nonanalytic (real) two-dimensional map. Magnifications of the "Cantor-like" structure at right angles to the diagonal and the ribs of the skeleton (cf. Fig. 5(a)) exhibit a stripe pattern with continuous boundaries (Fig. 5(b)). The pattern repeats at further magnifications.

Roessler et al. [4] mention an earlier example of a similar Julia boundary discovered by Mira [15] in the study of two different embedded periodic attractors coexisting in a cubic analogue to Hénon's map. Mira called the object "frontière floue" (fuzzy boundary); both basins were found to accumulate on a Cantor set. In [4], the authors themselves give an almost trivial example of continuous Julia-like boundaries with noninvertible (real) two-dimensional maps; they studied two uncoupled logistic maps in the "exploded" (chaotic) case.

Almost totally disconnected ("Cantor-like") seems to be the Julia boundary in the second case,

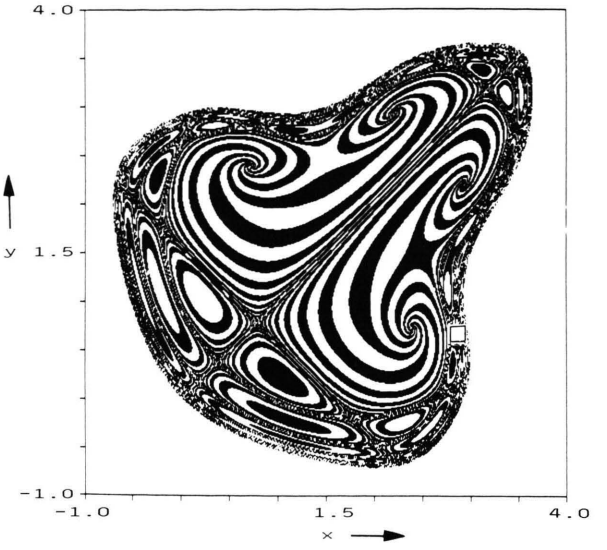

a)

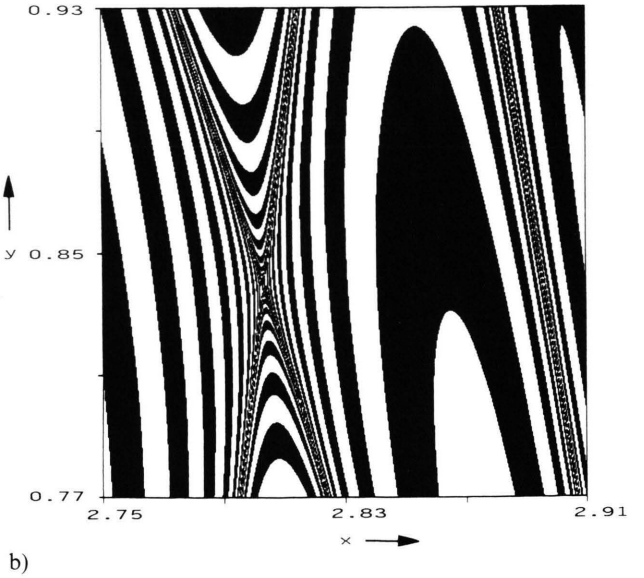

b)

Fig. 5. (a) Basins of the two coexisting period-10 orbits at $h = 0.645$ (cf. next figure). $480 \cdot 480$ initial points in the region $[-1, 4] \times [-1, 4]$ have been iterated under (4) with max. 2000 steps. If an orbit gets closer than 10^{-4} to a selected member of the first period, the pixel corresponding to its initial value is coloured black. All other initial values remain white. The white mirror image of the black basin is the basin of the other period-10 orbit. – (b) Increased resolution of Fig. 5(a) with $480 \cdot 480$ points out of the set $[2.75, 2.91] \times [0.77, 0.93]$. We note a stripe structure that repeats at further magnifications of the "Cantor-like" regions.

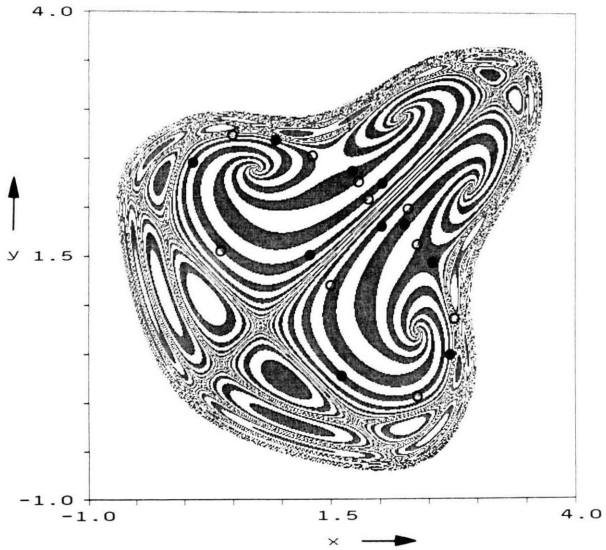

Fig. 6. Two types of period-10 orbits at $h = 0.645$. Filled and punched dots denote one stable and one unstable orbit, respectively. Not in the figure are their mirror images. A selected member of the stable orbit is approximately given by (1.883385, 2.162491) and for the unstable case by $(4.212209 \cdot 10^{-1}, 1.495815)$.

$h = 0.678$ (Figure 7 (a)). Now two symmetric $p = 15$ attractors coexist with one $p = 26$ attractor. Not distinguishing in Fig. 7 between the two $p = 15$ orbits, we obtain two basins separated again by a continuous Julia set as the stripe pattern in the blow up (Fig. 7 (b)) suggests to us. The stripe pattern repeats at suitable magnifications. This self-similar stripe structure formed by the basins of coexisting attractors has already been discovered by Kaneko [2], who studied the basins of two coexisting 32-cycles.

5. Julia-Like Behavior in the Parameter Space

Roessler et al. [4] predict that all potentially hyperchaotic systems (in [2] Kaneko found hyperchaos for the coupled logistic map) ought to possess Julia-like behavior in their parameter spaces. Indeed, (4) provides examples to support this presumption, when we extend the map by two passive additive variables c_x (first equation) and c_y, or when we explore it in the two-dimensional (h_x, h_y)-parameter space instead of $h_x = h_y = h$. Specifically, we considered the map

$$\begin{aligned} x_{k+1} &= x_k + h_x(x_k - x_k^2 + y_k + c_x)\,, \\ y_{k+1} &= y_k + h_y(y_k - y_k^2 + x_k + c_y)\,. \end{aligned} \tag{19}$$

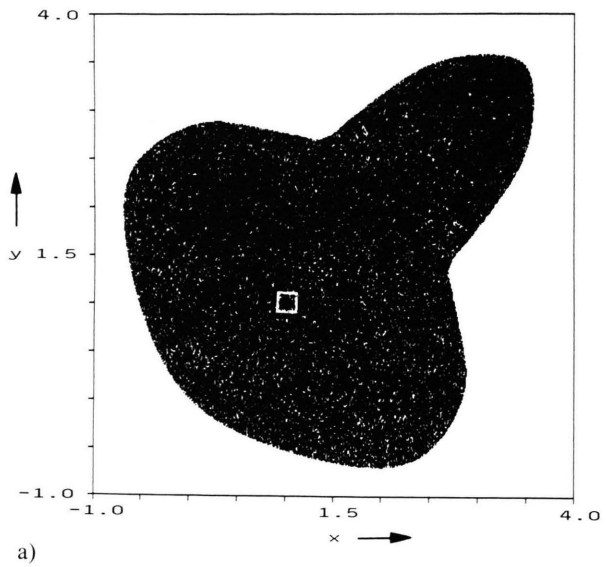

a)

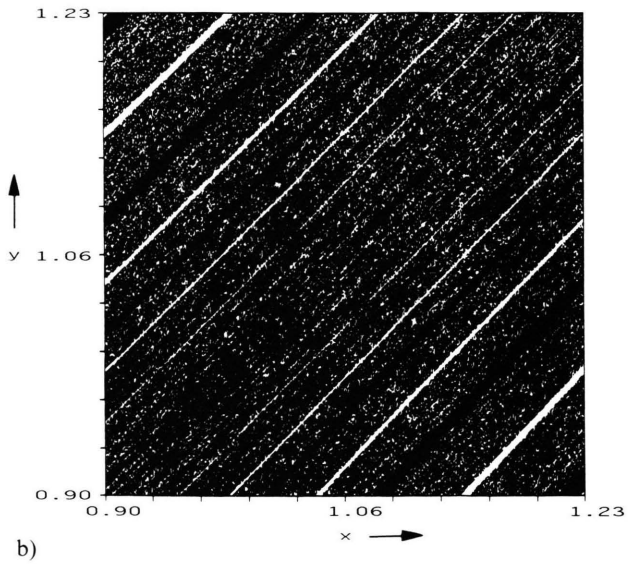

b)

Fig. 7. (a) Basins of a period-26 attractor of (4) coexisting with two period-15 attractors at $h = 0.678$. Plotting convention, data and detail like Figure 6. Pixels corresponding to basin points of the period-26 orbit are painted black. – (b) Increased resolution of Fig. 7 (a) with $480 \cdot 480$ initial points in $[0.9, 1.23] \times [0.9, 1.23]$. We note continuous Julia-boundaries of the basins.

First, for $c_x = c_y = 0.1$ and $h_x = h_y = 0.684$ (in the chaotic region) we computed an analogous "speed pattern" in the phase space as described for the original coupled map (4) in the preceding section (Figure 8). In contrast to Fig. 3, now all black and white level sets are niveaus of equal speed of divergence. But the skeleton persists, and when we

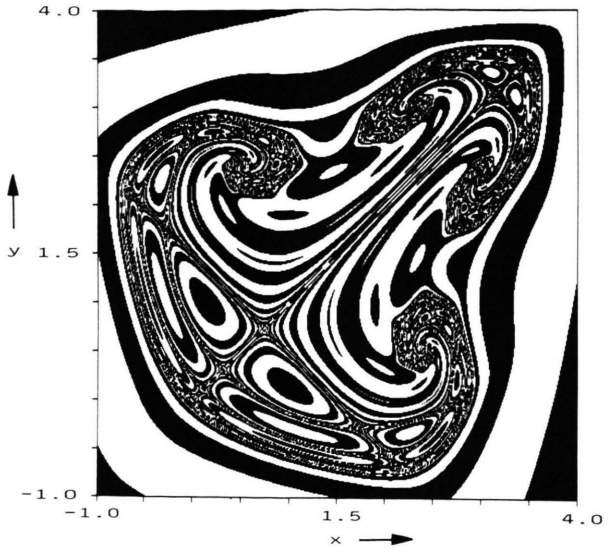

Fig. 8. Level sets of equal speed of divergence of the map (19) in the phase space at $c_x = c_y = 0.1$ and $h_x = h_y = 0.684$. For $480 \cdot 480$ initial points (pixels) in the region $[-1, 4] \times [-1, 4]$ the map has been iterated until $x_k^2 + y_k^2$ exceeds a given boundary $S = 10\,000$. Pixels iterates of which exceed S for the first time at an odd number of iteration steps are painted black.

Fig. 9. Detail from the (c_x, c_y)-parameter space with $4.095 \leqq c_x \leqq 4.135$, and $4.091 \leqq c_y \leqq 4.139$, $x_0 = y_0 = 0$ and $h_x = h_y = 0.684$. Level set colouring follows the description of Fig. 8, but now the iteration scheme (19) has been applied to a matrix of $4096 \cdot 5120$ initial points. Computation of this figure has been performed on IBM 4361-5, graphical representation on IBM 4250.

blow up the "hooks" of the anchor structure in Fig. 8, the self-similar features repeat in a very striking manner.

Similar computergraphical experiments (following techniques of Peitgen and Richter [16] f. e.) with (19) in the (c_x, c_y)- and in the (h_x, h_y)-parameter space can be found in [17]. All of them show self-similar repetitions of pattern at appropriate magnifications, but no fractal boundaries as known from [16]. Especially, exploring the map (19) in the (c_x, c_y)-parameter space for $x_0 = y_0 = 0$ and again $h_x = h_y = 0.684$ results in self-similarities given by Figure 9. The "face" which is a detail of a basic structure looking like a frog [17] exhibits remarkable self-similarities – now in a parameter space.

6. Complex Continuation

Due to the relation between the (complex) Mandelbrot set and the (real) period doubling scenario of Feigenbaum it is near at hand to regard the complex version of (4), i. e. the system

$$\begin{aligned} \mathrm{re}\,(x_{n+1}) &= \mathrm{re}\,(x_n) + h\,(\mathrm{re}\,(x_n) \\ &\quad - \mathrm{re}\,(x_n)^2 + \mathrm{im}\,(x_n)^2 + \mathrm{re}\,(y_n))\,, \\ \mathrm{im}\,(x_{n+1}) &= \mathrm{im}\,(x_n) + h\,(\mathrm{im}\,(x_n) \\ &\quad - 2\,\mathrm{re}\,(x_n)\,\mathrm{im}\,(x_n) + \mathrm{im}\,(y_n))\,, \\ \mathrm{re}\,(y_{n+1}) &= \mathrm{re}\,(y_n) + h\,(\mathrm{re}\,(y_n) \\ &\quad - \mathrm{re}\,(y_n)^2 + \mathrm{im}\,(y_n)^2 + \mathrm{re}\,(x_n))\,, \\ \mathrm{im}\,(y_{n+1}) &= \mathrm{im}\,(y_n) + h\,(\mathrm{im}\,(y_n) \\ &\quad - 2\,\mathrm{re}\,(y_n)\,\mathrm{im}\,(y_n) + \mathrm{im}\,(x_n))\,. \end{aligned} \tag{20}$$

We outline some results of experiments in two-dimensional subspaces of the four-dimensional phase space of (20) with $h = 0.645$. The first subspace is obtained by varying $\mathrm{re}\,(x_0)$ and $\mathrm{im}\,(x_0)$ and setting $\mathrm{re}\,(y_0) = \mathrm{re}\,(x_0)$ and $\mathrm{im}\,(y_0) = 0$. Figure 10 (a) represents all initial points in this subspace with bounded orbits, looking like "Mandelbrot-streets". These streets pass through single points of the middle horizontal given by $\mathrm{im}\,(x) = 0$. Thus this

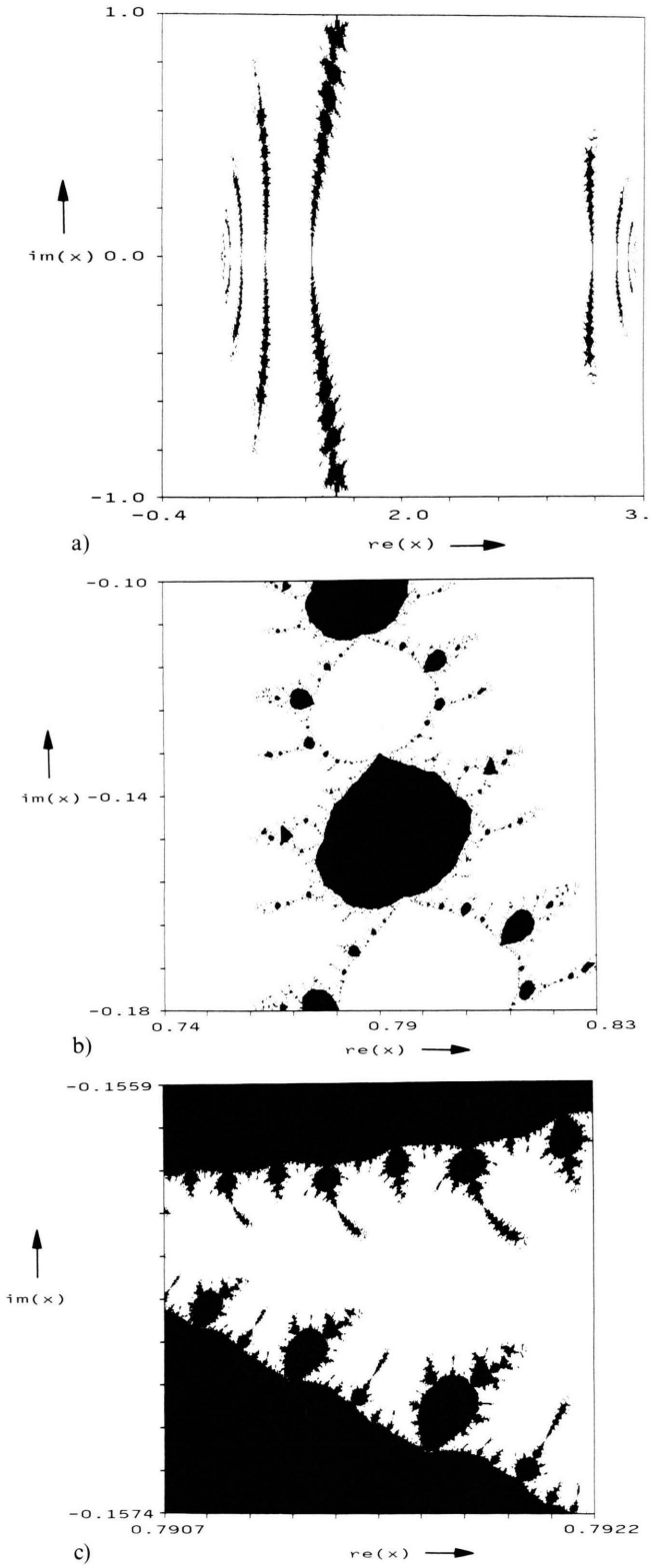

line is characterized by $\mathrm{re}(x) = \mathrm{re}(y)$, $\mathrm{im}(x) = 0$ and $\mathrm{im}(y) = 0$, i. e. it corresponds to the diagonal of the pear in Figure 4. In fact, it turns out that the intersection points between the complex streets and the middle horizontal in Fig. 10 (a) coincide with the real intersection points between the skeleton and the diagonal in Figure 4.

The next experiments examine the bounded orbits more precise. It turns out that even in the complex continuation all initial points with bounded orbits belong to the basins of attractin of the two period-10 orbits, known from the real case. Figure 10 (b) is a detail of Fig. 10 (a) and shows one of these basins. The clusters of the streets belong alternately to the two basins, not only on the main streets, but also on the side-streets. The fractal boundaries of the basins are demonstrated more detailed in Figure 10 (c). The boundary points of Fig. 10 (b) are classical three corner points forming the common boundary of the basins of either period-10 orbit and infinity.

A second two-dimensional subspace of the phase space of (20) is illustrated in Figure 11. It indicates the convergence behaviour by varying $\mathrm{re}(x_0)$ and $\mathrm{re}(y_0)$ with $\mathrm{im}(x_0) = \mathrm{im}(y_0) = 0.01$. The black region represents convergency (to the two stable period-10 orbits) and the other points inside the pear can easily be associated with the skeleton and the separatrix of the basins of attraction of the period-10 orbits (cf. Figures 4, 5). This connection can be observed still closer with smaller constants $\mathrm{im}(x_0) = \mathrm{im}(y_0)$.

7. Conclusion

Formerly [13], the fascinating structure of the chaotic attractor at $h = 0.684$ (cf. Fig. 1) captivated

Fig. 10. (a) The region $[-0.4, 3.6] \times [-1, 1]$ out of a two-dimensional subspace (for details see text) of the four-dimensional phase space of (20). It presents at $h = 0.645$ all initial points with bounded orbits. The black points are those out of $480 \cdot 480$ which do not leave a circle of radius 100 around (0, 0) within a maximum of 2000 iterations. – (b) Increased resolution of Fig. 10 (a) with $480 \cdot 480$ initial points in $[0.74, 0.83] \times [-0.18, -0.1]$. The basin of attraction of one of the period-10 orbits is marked. For numerical details cf. Figure 5 (a). (c) A detail of Figure 10 (b). Within the region $[0.7907, 0.7922] \times [-0.1574, -0.1559]$ the black points are those which belong to the basins of either of the two attracting period-10 orbits at $h = 0.645$.

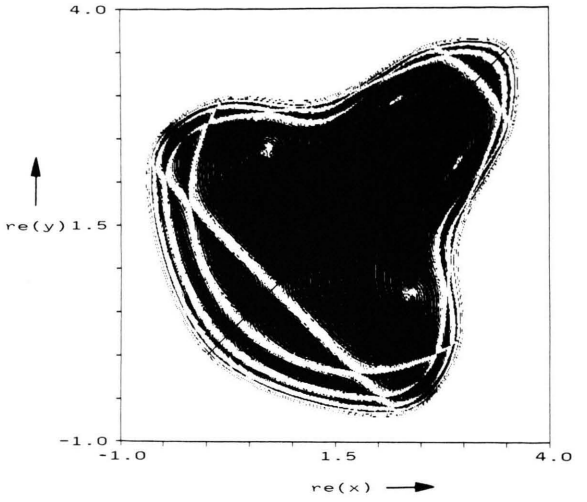

Fig. 11. The region $[-1, 4] \times [-1, 4]$ out of a two-dimensional subspace (for details see text) of the four-dimensional phase space of (20). It represents at $h = 0.645$ all initial points with bounded orbits. The black points are those out of $480 \cdot 480$ which do not leave a circle of radius 100 around $(0, 0)$ within a maximum of 2000 iterations.

us. Now, the richness of structure in the state and in the parameter space of (4) holds our interest. The coupled logistic map is not only a good model to study the dynamics of driven coupled oscillators [3], but also a canonical example of a nonanalytical (real) two-dimensional map with both self-similarities formed by the basins of attraction of coexisting cycles and Julia-like boundaries [4].

To recapture a classical continuous Julia set in 2D, one has to proceed (the next) higher dimension after [4]. In the last section, we took another way as proposed there. We regarded two-dimensional subspaces of the four-dimensional phase space of the complex continuation (20). Experiments demonstrate fractal boundaries of the basins in these subspaces with a close connection to the phenomena in the real case.

Many questions remain open. For example, it would be nice to be able to explain the conspicuous similarity between the Julia-like pattern in the basins of coexisting periodic attractors (Fig. 5) and the black/white level set colouring of the "speed patterns" in Figs. 3 and 8, respectively. Or in agreement with [4], to observe the described phenomena for other two-dimensional real maps. Are these properties universal?

Acknowledgements

We thank Professor Otto E. Roessler for stimulations and IBM Deutschland for computer graphics facilities. – Elaboration of a paper presented at the "Workshop on Symmetry" organized by Jürgen Parisi at the Darmstadt Symmetry Conference, June 1986.

[1] P. Collet and J.-P. Eckmann, Iterated Maps on the Interval as Dynamical Systems, A. Jaffe and D. Ruelle (eds.), Birkhäuser, Basel 1980.
[2] K. Kaneko, Prog. Theor. Phys. **69,** 1427 (1983).
[3] T. Hogg and B. A. Huberman, Phys. Rev. **29 A,** 275 (1984).
[4] O. E. Roessler, C. Kahlert, J. Parisi, J. Peinke, and B. Röhricht, Z. Naturforsch. **41 a,** 819 (1986).
[5] M. Prüfer, Siam J. Appl. Math. **45,** 32 (1985).
[6] M. Feigenbaum, J. Stat. Phys. **21,** 669 (1979).
[7] T. Y. Li and J. A. Yorke, Amer. Math. Monthly **82,** 985 (1975).
[8] R. B. May, Nature London **261,** 459 (1976).
[9] I. Waller and R. Kapral, Phys. Rev. **30 A,** 2047 (1984).
[10] J. Frøyland, Physica **8 D,** 423 (1983).
[11] R. R. Whitehead and N. MacDonald, Physica **13 D,** 401 (1984).
[12] J. Guckenheimer and P. Holmes, Nonlinear Oscillations, Dynamical Systems and Bifurcations of Vector Fields, Springer, New York 1986.
[13] W. Beau, W. Metzler, and A. Ueberla, The Route to Chaos of Two Coupled Logistic Maps, Dynamics Days, La Jolla, January 7–10, 1986, Preprint.
[14] O. E. Roessler, J. L. Hudson, and J. A. Yorke, Z. Naturforsch. **41 a,** 979 (1986).
[15] C. Mira, C. R. Acad. Sci. Paris A **288,** 591 (1979).
[16] H. O. Peitgen and P. H. Richter, Ber. Bunsenges. Phys. Chemie **89,** 571 (1985) and Phys. Bl. **42,** 9 (1986).
[17] W. Beau, W. H. Hehl, and W. Metzler, Computerbilder als Hilfsmittel zur Analyse gekoppelter logistischer Gleichungen, to appear: Informatik – Forschung und Entwicklung.